Femtoscopic probes with strange particles in STAR

G. Nigmatkulov [a,1] *(for the STAR Collaboration)*

[a] National Research Nuclear University MEPhI, Moscow, 115409, Russia

Heavy-ion collisions provide information about the properties of the matter under extreme conditions. Measurement of strangeness production properties provides important information about the collision region evolution. The spatial and temporal characteristics of particle emission can be extracted using femtoscopy technique. The collision energy, centrality, and transverse mass dependence of the three-dimensional charged kaon femtoscopic radii for Au+Au collisions in the Beam Energy Scan program is presented.

PACS: 12.38.Mh, 25.75.Nq,

1. Introduction

The first phase of Beam Energy Scan program (BES-I) performed at the BNL Relativistic Heavy Ion Collider (RHIC) in 2010, 2011 and 2014 was dedicated to study features expected to appear in the Quantum Chromodynamics (QCD) phase diagram. At high energies it is shown [1] that the matter formed in the collision behaves as a hot and almost perfect fluid with low chemical potential, μ_B, and consists of deconfined quarks and gluons. The phase transition from this state of matter to hadrons is likely a rapid, smooth cross-over transition [2]. At lower energies μ_B becomes larger and lattice QCD predicts [3] a first-order phase transition. The relative amounts of time the matter spends in the different phases may imprint a signal on observables that are sensitive to the equation of state [4]. The correlation femtoscopy technique has been developed [5] to study space and time properties of the particle-emitting source based on quantum statistical (QS) correlations, the properties of the final-state interactions (FSI) [6], space-time asymmetries using unlike particles [7] and may be sensitive to the nature of phase transition [8].

In these proceedings, we present recent femtoscopy measurements with strange particles performed by the Solenoidal Tracker At RHIC (STAR) experiment.

2. Correlation function

The correlation femtoscopy method uses a two-particle correlation function, $C(q)$, that experimentally can be defined as a ratio of the two-particle spectrum from the same events, $N(q)$, and that from the mixed events, $D(q)$, where q is the momentum

[1] E-mail: nigmatkulov@gmail.com; ganigmatkulov@mephi.ru

difference between the first and second particle from the pair decomposed in the Bertsch-Pratt coordinate system [12] to q_{out}, q_{side} and q_{long} components. The source radii are extracted by the standard Bowler-Sinyukov [13] method to fit the correlation functions assuming the Gaussian shape of the correlation function:

$$C(q) = N\left[1 - \lambda + \lambda K(q_{inv}, R_{inv})\left(1 + \exp(-R_{out}^2 q_{out}^2 - R_{side}^2 q_{side}^2 - R_{long}^2 q_{long}^2)\right)\right], \tag{1}$$

where N is a normalization parameter, λ is a correlation strength and R_{out}, R_{side}, R_{long} are the Gaussian source radii, and $K(q_{inv}, R_{inv})$ is a Coulomb correction factor.

3. Kaon femtoscopy in BES

Femtoscopy is a standard method of studying space-time properties of the system created in heavy-ion collisions [9]. Usually femtoscopic analyses are performed using charged pions [10,11] as they are the most abundantly produced particles. The Au+Au collisions at $\sqrt{s_{NN}}$ = 7.7, 11.5, 14.5, 19.6, 27, 39, 62.4, and 200 GeV during the BES-I program make it possible to perform femtoscopic measurements with the heavier particles – kaons. In addition to the identification via specific ionization energy loss (dE/dx) in the Time Projection Chamber (TPC), the time-of-flight information from the Time-Of-Flight (TOF) detector was used to identify pions and kaons. This allowed to perform particle identification in a wide momentum range of $0.15 \leq p$ (GeV/c)≤ 1.45.

Figure 1 shows the STAR preliminary results on kaon femtoscopic radii from Au+Au collisions at $\sqrt{s_{NN}}$ = 200 GeV as a function of the centrality and the average pair transverse momentum, $k_T = |\vec{p_1} + \vec{p_2}|_T/2$, where $\vec{p_1}$ and $\vec{p_2}$ are the three-momentum of the first and second particle from pair, respectively.

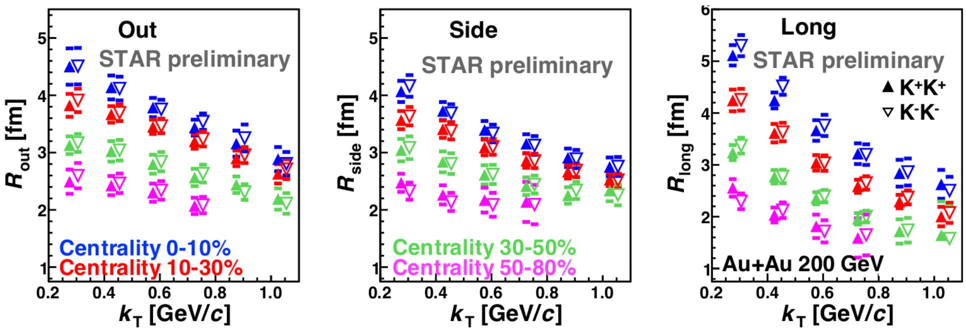

Fig. 1: The R_{out}, R_{side}, and R_{long} as a function of the pair transverse momentum, k_T, for positive (solid symbols) and negative (open symbols) kaon pairs for 4 centrality ranges: 0-10% (blue symbols), 10-30% (red symbols), 30-50% (green symbols), and 50-80% (magenta symbols). Shown results are for Au+Au collisions at $\sqrt{s_{NN}}$ = 200 GeV. Only statistical uncertainties shown.

The analysis was performed for 4 centrality intervals, namely 0-10% (blue symbols), 10-30% (red symbols), 30-50% (green symbols) and 50-80% (magenta symbols) central

Au+Au collisions and for 6 k_T bins. The correlation functions for positive and negative kaon pairs were constructed separately. The emitting-source radii for positive and negative kaons were found to be consistent within statistical uncertainties. The measured charged kaon source radii follow typical centrality and pair transverse momentum dependence. The system expansion and transverse flow cause the fall of R_{out} and R_{side} with increasing k_T, while the longitudinal expansion leads to the decrease of R_{long} with increasing k_T. Same exercise, with the same results, has been performed for lower collision energies.

Figure 2 shows a comparison of kaon (open stars) and pion (open triangles) source radii extracted for the 0-5% (blue symbols) and 30-40% (red symbols) central Au+Au collisions at $\sqrt{s_{NN}} = 200$ GeV. This analysis extended the previous pion femtoscopy results [11] (solid triangles) to higher transverse mass range, $m_T = \sqrt{m^2 + k_T}$, where k_T is the pair transverse momentum and m is a particle rest mass, by a factor of 2 using identification from both the TPC and TOF detectors. The R_{out} values for kaons are systematically larger than those of pions, while the R_{side} values for kaons and pions are comparable, and the m_T-dependence of R_{long} is different between kaons and pions.

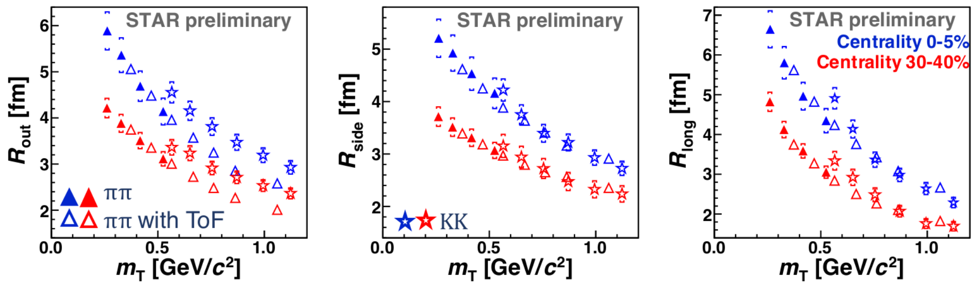

Fig. 2: The comparison of the kaon (stars) and pion (triangles) source radii from Au+Au collisions at $\sqrt{s_{NN}} = 200$ GeV in STAR. The solid triangles represent pion source radii taken from [11], open symbols show femtoscopic radii for pions and kaons identified using information from both the TPC and TOF detectors. Red and blue symbols show data for 0-5% and 30-40% central collision, respectively. Only statistical uncertainties shown.

Figure 3 shows the $\sqrt{s_{NN}}$ dependence of the pion and kaon femtoscopic radii, R_{out} (top panel), R_{side} (middle panel), and R_{long} (bottom panel). The extracted radii for both pions and kaons show smooth trend with increasing collision energy. The R_{out} and R_{side} show a small increase at the RHIC energies, and are slightly larger at the LHC. The values of R_{long} suggest that medium lives longer at the LHC as compared to RHIC.

4. Femtoscopy in the FXT program

In 2015 STAR conducted a fixed-target (FXT) test run using gold ion collisions at $\sqrt{s_{NN}} = 4.5$ GeV to show that STAR is capable to run in a fixed-target configuration. One beam was circulated in the collider and lowered to directly graze the edge of a 1 mm thick (4% interaction probability) gold foil target. The target was placed at the edge

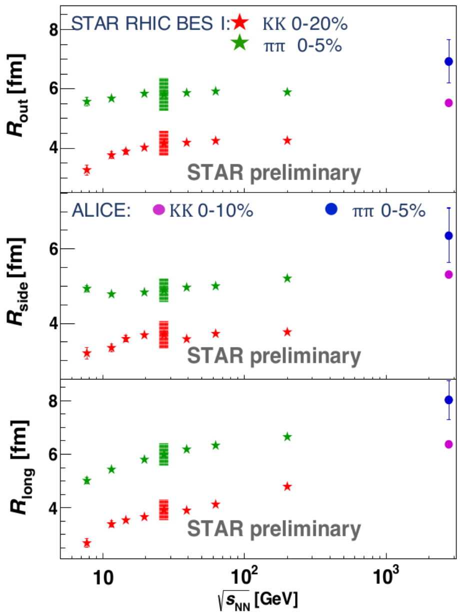

Fig. 3: Femtoscopic radii of pions (red stars) and kaons (green stars), R_{out} (top panel), R_{side} (middle panel), and R_{long} (bottom panel) as a function of collision energy, $\sqrt{s_{NN}}$. ALICE data for pions (blue) [14] and kaons (magenta) [15] are shown by circles. Shaded bands represent systematic uncertainty.

of the TPC, about 211 cm away from the center of the detector to make use of the full tracking volume of the TPC. Approximately 1.3 million events were collected with a top $\approx 30\%$ centrality trigger. Figure 4 (left) shows the measured femtoscopic radii as a function of transverse mass for 0-10% central Au+Au collisions in the fixed-target mode.

The STAR FXT results are compared with E895 [16] and E866 (E802) [17] and are consistent with the energy dependence trend of these other experiments within uncertainties. Figure 4 (right) shows the dependence of R_{side}, which reflects the transverse size of the source, on R_{long} that reflects the size in the longitudinal direction for several collision energies. As the collision energy increases in the FXT regime, compression reduces the source size and increases the baryon density, whereas the BES collider regime shows increasing longitudinal expansion.

5. Conclusions

In these proceedings, preliminary results from the STAR experiment on identical pion and kaon femtoscopy from Au+Au collisions at $\sqrt{s_{NN}} = 7.7$–200 GeV in the collider and $\sqrt{s_{NN}} = 4.5$ GeV in fixed-target (FXT) modes were presented. The kaon source radii R_{out} , R_{side} and R_{long} were extracted from the three-dimensional analysis for different collision centralities and pair transverse momenta. The extracted source radii show centrality and transverse pair momentum dependence typical for a collectively expanding source.

Acknowledgements

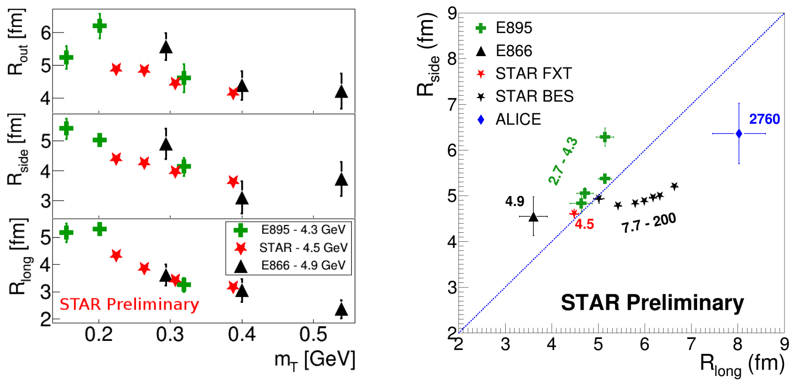

Fig. 4: (Left) Transverse mass dependence of R_{out}, R_{side}, and R_{long} for pions measured for 0-10% Au+Au collisions in STAR (red stars), E895 (black triangles) [16], and E866 (green crosses) [17]. (Right) The R_{side} vs. R_{long} dependence for the E866, E895, STAR and ALICE [14] experiments. Only statistical uncertainties shown.

The reported study was funded by RFBR according to the research project No. 16-02-01119a, partially supported the Ministry of Science and Higher Education of the Russian Federation, grant No 3.3380.2017/4.6, and by the National Research Nuclear University MEPhI in the framework of the Russian Academic Excellence Project (contract No. 02.a03.21.0005, 27.08.2013). The part of our work was performed using resources of NRNU MEPhI high-perfomance computing center.

REFERENCES

1. *Adams J. et al. (STAR Collab.)* // Nucl. Phys. A. 2005. V. 757. P. 102.; *Adcox K. et al.(PHENIX Collab.)* // Nucl. Phys. A. 2005. V. 757. P. 184.; *Back B. B. et al. (PHOBOS Collab.)* // Nucl. Phys. A. 2005. V. 757. P. 28.; *Arsene I. et al. (BRAHMS Collab.)* // Nucl. Phys. A. 2005. V. 757. P. 1.

2. *Aoki Y., Endrodi G., Fodor Z., Katz S., Szabo K.* // Nature. 2006. V. 443. P. 675.; *Borsanyi S. et al. (Wuppertal-Budapest Collab.)* // J. High Energy Phys. 2010. V. 09. P. 073.

3. *Halasz M. A., Jackson A. D., Shrock R. E., Stephanov M. A., Verbaarschot J. J. M.* // Phys. Rev. D. 1998. V. 58. P. 096007.; *Antoniou N. G., Kapoyannis A. S.* // Phys. Lett. B. 2003. V. 563. P. 165.

4. *Randrup J.* // Phys. Rev. C. 2010. V. 82. P. 034902.

5. *Kopylov G. I., Podgoretsky M. I.* // Sov. J. Nucl. Phys. 1972. V. 15. P. 219.; *Kopylov G. I.* // Phys. Lett. B. 1974. V. 50. P. 472.; *Podgoretsky M. I.* // Sov. J. Part. Nucl. 1989. V. 20. P. 266.

6. *Lednicky R., Lyuboshitz V. L.* // Sov. J. Nucl. Phys. 1982. V. 35. P. 770.

7. *Lednicky R. et al.* // Phys. Lett. B. 1996. V. 373. P. 30.

8. *Rischke D. H., Gyulassy M.* // Nucl. Phys. A. 1996. V. 608. P. 479.

9. *Lisa M. A., Pratt S., Soltz R., Wiedemann U.* // Ann. Rev. Nucl. Part. Sci. 2005. V. 55. P. 357.

10. *Adams J. et at. (STAR Collab.)* // Phys. Rev. C. 2005. V. 71. P. 044906.

11. *Adamczyk L. et al. (STAR Collab.)* // Phys. Rev. C. 2015. V. 92. P. 014904.

12. *Bertsch G., Gong M., Tohyama M.* // Phys. Rev. C. 1988. V. 37. P. 1896.; *Pratt S.* // Phys. Rev. D. 1986. V. 33. P. 1314.

13. *Bowler M.G.* // Phys. Lett. B. 1991. V. 270. P. 69.; *Sinyukov Yu., Lednicky R., Akkelin S.V., Pluta J., Erazmus B.* // Phys. Lett. B. 1998. V. 432. P. 248.

14. *Aamodt K. et al. (ALICE Collab.)* // Phys. Lett. B. 2011. V. 696. P. 328–337.

15. *Malinina L. (for ALICE Collab.)* // Nucl. Phys. A. 2016. V. 956. P. 373–376.

16. *Lisa M. A. et al. (E895 Collab.)* // Phys. Rev. Lett. 2000. V. 84. P. 2798.

17. *Ahle L. et al. (E866 Collab.)* // Phys. Rev. C. 2002. V. 66. P. 054906.